Front. Phys. 13(1), 130305 (2018)
DOI 10.1007/s11467-017-0711-9

Research article

Multipartite quantum correlations among atoms in QED cavities

J. Batle[1,†], A. Farouk[2], O. Tarawneh[3], S. Abdalla[4]

[1] *Departament de Física, Universitat de les Illes Balears, 07122 Palma de Mallorca, Balearic Islands, Spain*
[2] *Faculty of Computer and Information Sciences, Mansoura University, Egypt*
[3] *Information Technology Department, Al-Zahra College for Women, P.O. Box 3365, Muscat, Oman*
[4] *Department of Physics, Faculty of Science, King Abdulaziz University Jeddah, P.O. Box 80203. Jeddah 21589, Saudi Arabia*
Corresponding author. E-mail: †jbv276@uib.es
Received May 25, 2017; accepted June 4, 2017

We study the nonlocality dynamics for two models of atoms in cavity quantum electrodynamics (QED); the first model contains atoms in a single cavity undergoing nearest-neighbor interactions with no initial correlation, and the second contains atoms confined in n different and noninteracting cavities, all of which were initially prepared in a maximally correlated state of n qubits corresponding to the atomic degrees of freedom. The nonlocality evolution of the states in the second model shows that the corresponding maximal violation of a multipartite Bell inequality exhibits revivals at precise times, defining, *nonlocality sudden deaths* and *nonlocality sudden rebirths*, in analogy with entanglement. These quantum correlations are provided analytically for the second model to make the study more thorough. Differences in the first model regarding whether the array of atoms inside the cavity is arranged in a periodic or open fashion are crucial to the generation or redistribution of quantum correlations. This contribution paves the way to using the nonlocality multipartite correlation measure for describing the collective complex behavior displayed by slightly interacting cavity QED arrays.

Keywords quantum optics, cavity quantum electrodynamics, multipartite nonlocality

PACS numbers 03.65.Ud, 03.67.Mn

1 Introduction

The advent of quantum information theory (QIT) has paved the way to a deeper understanding not only of the nature of the correlations existing between different quantum systems, which are responsible for the improved performance of tasks or even the performance of tasks that have no classical counterpart, but also of the physics of composite quantum systems [1–3].

Quantum correlations lie at the heart of QIT. Among those correlations, entanglement is perhaps one of the most fundamental and nonclassical features exhibited by quantum systems [1, 1–9]. In addition, the maximum violation of a Bell inequality for n parties is a good figure of merit that complements entanglement in scenarios where the study of truly multipartite quantum correlations is somehow impossible [10, 11].

Long regarded as identical, entanglement and nonlocality constitute different quantum physical resources. They imply each other only in the simplest possible case of a pure state of two qubits, i.e., the celebrated *Gisin theorem* [12]. Remarkably, there are views such as Schumacher's [13] that do not conclude that quantum mechanics is nonlocal merely because a state violates a Bell inequality. Instead, Schumacher concludes that the message behind the violation of Bell inequalities by quantum states ρ is that quantum correlations cannot in general be shared by more than two parties.

There exist certain tasks, such as device-independent quantum key distribution [14–16] and quantum communication complexity problems [17], which can be performed or solved only if the corresponding entangled states exhibit *nonlocal correlations*. Nonlocality, as measured by the violation of Bell inequalities, describes the part of quantum correlations that cannot be reproduced by any classical local model. Nonlocality plays a key role in some applications of QIT [14–16] and in infinite quantum systems [10, 11], in which the violation of Bell inequalities can constitute a complementary resource and pinpoint the critical points associated with quantum phase transitions. Thus, the maximum violation of a Bell inequality (to be regarded simply as *nonlocality*) for an arbitrary number of parties is physically relevant *per se*, even if we do not address multipartite quantum entanglement, as in the present work.

The physical implementation of many concepts in QIT aims to utilize the quantum concepts of i) state superpositions and ii) entanglement or other quantum correlations in order to perform communication and computation operations that are impossible according to the tenets of mathematical logic.

An interesting experimental proposal along these lines is provided by cavity quantum electrodynamics (QED) experiments [18–22]. They deal with atom–photon interactions in a fully quantum mechanical way, with atom–atom interactions playing a minor role. Cavity QED has been traditionally developed as an area of fundamental research in light–matter interactions. In fact, a paradigmatic exactly solvable model in this field is the celebrated Jaynes–Cummings (JC) model [23, 24]. The JC model describes the interaction of a single two-level atom with a single-mode cavity field.

One of the principal aims of cavity QED studies is to gain extraordinary control over atomic and photonic states for fundamental and quantum information studies [25–30]. This is accomplished by controlling the spontaneous emission processes of atoms using a cavity.

Applications of cavity QED systems to quantum information processing derive mostly from the ability to coherently interconvert quantum states between material qubits and photon qubits. Using this basic primitive, many two-qubit gate protocols have been developed for creating atom–photon, atom–atom, or photon–photon entanglement correlations [31–35].

It is precisely the aim of the present work to study these correlations from the perspective of the maximal violation of Bell inequalities for an arbitrarily large number of parties. Here we study two models. In the first one, the "parties" are considered to be interacting atoms confined inside a single cavity, to which they are coupled. The second model treats the parties as separate noninteracting QED cavities, each containing one atom.

We will shed some light on the role of multipartite quantum correlation measures during the time evolution of these models. The present contribution is organized as follows. In Section 2, we introduce the cavity QED models described above and solve them analytically in utmost detail. The nonlocality measure employed during the time evolution is introduced in Section 3. The results for both models are presented in Section 4. The limitations on practical implementation of the systems studied are discussed in Section 5. Finally, some conclusions are drawn in Section 6.

2 Atoms in QED cavities

One of the few exactly solvable models in quantum physics for bipartite interaction, that is, the JC model [23, 24], has been exploited for studying the dynamics of entanglement [36, 37]. In an ideal cavity QED experiment, the atom can be viewed as a two-level system ($|g\rangle$ and $|e\rangle$) coupled to a single mode of the field, and the system evolution is determined by the famous JC Hamiltonian of quantum optics. Here we extend it to the multipartite case for two major models of atoms inside QED cavities.

As we shall see, specific initial states for both the cavity and atomic degrees of freedom are considered. These states give rise to the time evolution of the nonlocality measure in a specific way. Therefore, changing the initial state may imply a different evolution of these degrees of freedom. However, we choose the initial form of these states because the outcome exhibits interesting features. Further, our choice of initial state enables us to compute the evolution of the system analytically, either for an arbitrary number of atoms inside a cavity or for an arbitrary number of QED cavities.

A systematic study of different types of initial states would certainly render the following work more complete. In any case, and as a first approximation to systems of QED cavities, we believe that the present study with the current initial states is sufficiently representative.

2.1 Interacting atoms coupled to a single QED cavity

Let us suppose that n two-level atoms are trapped in a single-mode optical cavity, which possesses the field modes $\{|0\rangle, |1\rangle\}$, that is, the vacuum and an additional mode. We consider that each atom interacts with the cavity field. Thus, the interaction Hamiltonian in the rotating wave approximation reads as

$$H_I = \sum_{i=1}^{n} \left(g\left[a s_i^+ + a^+ s_i^- \right] + J\left[s_i^+ s_{i+1}^- + s_i^- s_{i+1}^+ \right] \right). \quad (1)$$

As usual, a^+ and a^- are the creation and annihilation operators of the cavity field, respectively, and $s_i^+ = |e\rangle_i\langle g|$ ($s_i^- = |g\rangle_i\langle e|$) are the atomic raising (lowering) operators for atoms $i = 1 \cdots n$. The coupling constant for each atom to the field is set to g, which has the same value for all of them, as does the atom–atom coupling coefficient J (nearest-neighbor interaction only). Thus, the pair $\{g, J\}$ determines the dynamics of the time evolution of Hamiltonian (1). We consider mostly periodic boundary

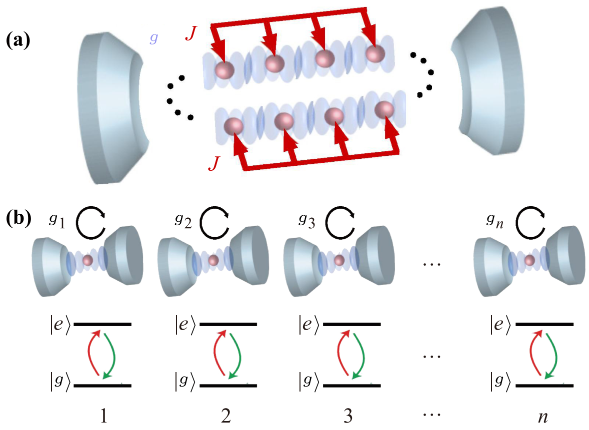

Fig. 1 Schematic plot of the two models considered in this work involving atoms and QED cavities. **(a)** First model (1), where atoms form a chain with an interatomic coupling J between nearest neighbors, all of them embedded in a single cavity with an atom–field interaction given by g. The configuration has periodic boundary conditions, although an open array is considered for $n = 3$ atoms. **(b)** Second model (13), where we have n two-level atoms, each inside a QED cavity and interacting only with the field mode via the couplings g_i. The cavities and atoms do not interact, although we consider that all initial atomic degrees of freedom are prepared in a maximally correlated Greenberger–Horne–Zeilinger (GHZ) state. See text for details.

conditions such that $s^{\pm}_{i+1} = s^{\pm}_1$, but one case ($n = 3$) is considered as a linear chain for comparison. The model is depicted schematically in Fig. 1(a).

Let us consider, for instance, the case of $n = 4$ atoms, with the initial state given by

$$|\Phi_{ABCDa}(t\!=\!0)\rangle = \big(\cos\alpha|gggg\rangle\otimes|0\rangle + \sin\alpha|gggg\rangle\otimes|1\rangle\big), \tag{2}$$

where A, B, C, and D stand for the four atoms, and a is the degree of freedom of the cavity field.

In the initial state of the four atoms inside the cavity, all the atoms remain in their respective ground states, and the field mode can be either $|0\rangle$ or $|1\rangle$. The first term does not evolve with time; thus, $c_0(t) = \cos\alpha$, whereas the second one does, so the total number of excitations is preserved (one in total). The subset of all states of the atoms plus cavity modes that become accessible is given by $\{|gggg1\rangle, |ggge0\rangle, |ggeg0\rangle, |gegg0\rangle, |eggg0\rangle\}$. Therefore, the evolved state has the following form:

$$\begin{aligned}|\Phi_{ABCDa}(t)\rangle &= c_0|gggg0\rangle + c_1|gggg1\rangle + c_2|ggge0\rangle \\ &\quad + c_3|ggeg0\rangle + c_4|gegg0\rangle + c_5|eggg0\rangle,\end{aligned} \tag{3}$$

with the initial conditions $c_1(0)=\sin\alpha$ and $c_2(0)=c_3(0)=c_4(0) = c_5(0) = 0$. The solution of the corresponding time-dependent Schrödinger equation now depends on whether periodic boundary conditions are considered.

The time evolution of $|\Phi_{ABCDa}(t)\rangle$ (3) is governed, in atomic units, by

$$\mathrm{i}\frac{\partial|\Phi_{ABCDa}(t)\rangle}{\partial t} = H_I|\Phi_{ABCDa}(t)\rangle. \tag{4}$$

2.1.1 Arrangement with periodic boundary conditions

Equating the basis states $\{|gggg1\rangle, |ggge0\rangle, |ggeg0\rangle, |gegg0\rangle, |eggg0\rangle\}$ on both sides of Eq. (4) returns the following set of differential equations:

$$\begin{aligned}\mathrm{i}\dot{c_1}(t) &= gc_2(t) + gc_3(t) + gc_4(t) + gc_5(t), \\ \mathrm{i}\dot{c_2}(t) &= gc_1(t) + Jc_3(t) + Jc_5(t), \\ \mathrm{i}\dot{c_3}(t) &= gc_1(t) + Jc_2(t) + Jc_4(t), \\ \mathrm{i}\dot{c_4}(t) &= gc_1(t) + Jc_3(t) + Jc_5(t), \\ \mathrm{i}\dot{c_5}(t) &= gc_1(t) + Jc_2(t) + Jc_4(t).\end{aligned} \tag{5}$$

Upon closer inspection, the previous set of differential equations reveals a substructure from $c_2(t)$ to $c_5(t)$: The permutation of the indices reveals that the coefficients $c_{2\cdots(n+1)}(t)$ are all equal (with the same initial condition). In fact, this result applies to the general case for n atoms inside the cavity interacting with each other with periodic boundary conditions. For n atoms, we have a set of $n+1$ differential equations with initial conditions $c_1(0) = \sin\alpha$ and $c_{2\cdots(n+1)}(0) = 0$, where only two solutions are different, $c_1(t)$ and $c_2(t)$ (the remaining ones are $c_{3\cdots(n+1)}(t) = c_2(t)$).

Therefore, we can now address the general n case by solving only two linear differential equations:

$$\begin{aligned}\mathrm{i}\dot{c_1}(t) &= ngc_2(t), \\ \mathrm{i}\dot{c_2}(t) &= gc_1(t) + 2Jc_2(t).\end{aligned} \tag{6}$$

The corresponding solutions for $c_1(t)$ and $c_2(t)$ that fulfill the set of initial conditions are given by

$$\begin{aligned}c_1(t) &= \frac{\sin\alpha}{\Delta}\mathrm{e}^{-\mathrm{i}Jt}\big[\mathrm{i}J\sin(\Delta t) + \Delta\cos(\Delta t)\big], \\ c_2(t) &= -\mathrm{i}\frac{g\sin\alpha}{\Delta}\mathrm{e}^{-\mathrm{i}Jt}\sin(\Delta t),\end{aligned} \tag{7}$$

where $\Delta \equiv \sqrt{J^2 + ng^2}$. The relevant values of the reduced density matrix for the atomic degrees of freedom depend, as we shall see, only on $c_0(t) = \cos\alpha$ and $|c_2|^2 = \frac{g^2\sin^2\alpha}{\Delta^2}\sin^2(\Delta t)$. A more compact way to express c_1 is $|c_1(t)|^2 = \frac{J^2 + n\,g^2\cos^2(\Delta t)}{\Delta^2}$. Notice that for the critical line $J \propto g$, $|c_1(t)|^2$ and $|c_2(t)|^2$ depend only on either J or g via the frequency Δ.

The evolved state is spanned in a basis that contains only one excitation:

$$\begin{aligned}|\Phi_{1..(n+1),a}(t)\rangle &= c_0|gg..gg0\rangle + c_1|gg..gg1\rangle + c_2|gg..ge0\rangle \\ &\quad + c_3|gg..eg0\rangle + \cdots + c_n|ge..gg0\rangle \\ &\quad + c_{n+1}|eg..gg0\rangle.\end{aligned} \tag{8}$$

The corresponding reduced density matrix is expressed in the basis of $n+1$ elements $\{|ggg..gg\rangle, |ggg..ge\rangle, \cdots, |gge..gg\rangle, |geg..gg\rangle, |egg..gg\rangle\}$, which is that of the generalized W states plus the initial basis element $|ggg..gg\rangle$. These atomic density matrices have a rank of $(n+1)$, which is certainly very small compared to the total dimension 2^n.

After some algebra, and taking into account normalization and the fact that $c_{3\cdots(n+1)}(t) = c_2(t)$, the general form of the nonzero elements of the reduced density matrix for the atomic degrees of freedom of n atoms interacting with each other inside a QED cavity with periodic boundary conditions reads as

$$\rho_{1..n}(t) = \begin{pmatrix} 1-n|c_2(t)|^2 & \cos\alpha c_2^*(t) & \cos\alpha c_2^*(t) & \dots & \cos\alpha c_2^*(t) & \cos\alpha c_2^*(t) & \dots & \cos\alpha c_2^*(t) & \cos\alpha c_2^*(t) & \cos\alpha c_2^*(t) \\ \cos\alpha c_2(t) & |c_2(t)|^2 & |c_2(t)|^2 & \dots & |c_2(t)|^2 & |c_2(t)|^2 & \dots & |c_2(t)|^2 & |c_2(t)|^2 & |c_2(t)|^2 \\ \cos\alpha c_2(t) & |c_2(t)|^2 & |c_2(t)|^2 & \dots & |c_2(t)|^2 & |c_2(t)|^2 & \dots & |c_2(t)|^2 & |c_2(t)|^2 & |c_2(t)|^2 \\ \vdots & \vdots & \vdots & \ddots & \vdots & \vdots & \iddots & \vdots & \vdots & \vdots \\ \cos\alpha c_2(t) & |c_2(t)|^2 & |c_2(t)|^2 & \dots & |c_2(t)|^2 & |c_2(t)|^2 & \dots & |c_2(t)|^2 & |c_2(t)|^2 & |c_2(t)|^2 \\ \cos\alpha c_2(t) & |c_2(t)|^2 & |c_2(t)|^2 & \dots & |c_2(t)|^2 & |c_2(t)|^2 & \dots & |c_2(t)|^2 & |c_2(t)|^2 & |c_2(t)|^2 \\ \vdots & \vdots & \vdots & \iddots & \vdots & \vdots & \ddots & \vdots & \vdots & \vdots \\ \cos\alpha c_2(t) & |c_2(t)|^2 & |c_2(t)|^2 & \dots & |c_2(t)|^2 & |c_2(t)|^2 & \dots & |c_2(t)|^2 & |c_2(t)|^2 & |c_2(t)|^2 \\ \cos\alpha c_2(t) & |c_2(t)|^2 & |c_2(t)|^2 & \dots & |c_2(t)|^2 & |c_2(t)|^2 & \dots & |c_2(t)|^2 & |c_2(t)|^2 & |c_2(t)|^2 \\ \cos\alpha c_2(t) & |c_2(t)|^2 & |c_2(t)|^2 & \dots & |c_2(t)|^2 & |c_2(t)|^2 & \dots & |c_2(t)|^2 & |c_2(t)|^2 & |c_2(t)|^2 \end{pmatrix}. \tag{9}$$

Recall that the previous density matrix $\rho_{1..n}(t)$ has rank $n+1$ and is given in the basis $\{|ggg..gg\rangle, |ggg..ge\rangle, \cdots, |gge..gg\rangle, |geg..gg\rangle, |egg..gg\rangle\}$, which is of course *not* the computational basis, although it is embedded in it. The purity of $\rho_{1..n}(t)$ can be calculated as

$$1/R = 1 - 2n|c_2(t)|^2\big(\sin^2\alpha - n|c_2(t)|^2\big). \tag{10}$$

The term in parentheses in (10) is always positive, so $R \geq 1$. In addition, this term is small, so the first correction to R can be obtained as $R \approx 1 + 2n|c_2(t)|^2\big(\sin^2\alpha - n|c_2(t)|^2\big)$. Therefore, we have that the ensuing states will always be either pure or slightly mixed, with a degree of mixture that departs from pure states according to the expression $2n|c_2(t)|^2\big(\sin^2\alpha - n|c_2(t)|^2\big)$.

From inspection, it is tantalizing to find those times where the term in parentheses in (10) is null, and thus $\rho_{1..n}(t)$ becomes a pure state. One can see that this condition would imply $\sin^2(\Delta t) = 1 + \frac{J^2}{ng^2}$, which is certainly impossible. However, it is remarkable that in the following three limits,

- $J = 0$ (no interatomic interaction), with $c_2(t) = -\mathrm{i}\frac{\sin\alpha}{\sqrt{n}}\sin(\sqrt{n}gt)$,
- $g \to \infty$ (extremely high coupling to the cavity), with $c_2(t) \approx -\mathrm{i}\frac{\sin\alpha}{\sqrt{n}}\mathrm{e}^{-\mathrm{i}Jt}\sin(\sqrt{n}gt)$,
- and $n \to \infty$ (many atoms in the cavity), with $c_2(t) \approx -\mathrm{i}\frac{\sin\alpha}{\sqrt{n}}\mathrm{e}^{-\mathrm{i}Jt}\sin(\sqrt{n}gt)$,

$\rho_{1..n}(t)$ becomes close to a pure state for $\Delta t^* = \frac{\pi}{2}, \frac{3\pi}{2}$ and other multiples for times t^*. Whereas for no interaction between atoms the expression for $c_2(t)$ is exact, the two latter limits imply very high oscillation frequencies and a J, g dependence of the results involving $\rho_{1..n}(t)$ [(9)].

However, the state of all atoms (9) becomes *exactly* a pure one whenever $c_2(t) = 0$, that is, when $\sin(\Delta t) = 0$. Thus, for times such as $\Delta t' = \pi, 2\pi, 3\pi\cdots$, the system evolves toward the same initial state at $t = 0$ s.

2.1.2 Arrangement with open boundary conditions

In this case, and equating again the basis states $\{|gggg1\rangle, |ggge0\rangle, |ggeg0\rangle, |gegg0\rangle, |eggg0\rangle\}$ on both sides of Eq. (4), we now obtain instead the following set of differential equations:

$$\begin{aligned} \mathrm{i}\dot{c}_1(t) &= gc_2(t) + gc_3(t) + gc_4(t), \\ \mathrm{i}\dot{c}_2(t) &= gc_1(t) + Jc_3(t), \\ \mathrm{i}\dot{c}_3(t) &= gc_1(t) + Jc_2(t) + Jc_4(t), \\ \mathrm{i}\dot{c}_4(t) &= gc_1(t) + Jc_3(t). \end{aligned} \tag{11}$$

The corresponding expression for the general g, J solution is rather involved. It is greatly simplified for the special case $J = g$. From inspection, and because the usual initial conditions are applied, we have $c_4(t) = c_2(t)$, which is indeed the case:

$$c_1(t) = -1/(34\mathrm{i})\big(17\mathrm{i}\mathrm{e}^{\mathrm{i}gt} + \sqrt{17}\mathrm{e}^{-1/(2\mathrm{i}gt)}\sin(1/(2\sqrt{17}gt)) + 17\mathrm{i}\mathrm{e}^{-1/2\mathrm{i}gt}\cos(1/2\sqrt{17}gt)\big)\sin\alpha,$$
$$c_2(t) = -2/(17\mathrm{i})\sqrt{17}\sin\alpha\mathrm{e}^{-1/(2\mathrm{i}gt)}\sin(1/(2\sqrt{17}gt)),$$
$$c_3(t) = -1/34\mathrm{i}\big(-17\mathrm{i}\mathrm{e}^{\mathrm{i}gt} + \sqrt{17}\mathrm{e}^{-1/(2\mathrm{i}gt)}\sin(1/(2\sqrt{17}gt)) + 17\mathrm{i}\mathrm{e}^{-1/2\mathrm{i}gt}\cos(1/2\sqrt{17}gt)\big)\sin\alpha,$$
$$c_4(t) = -2/(17\mathrm{i})\sqrt{17}\sin\alpha\mathrm{e}^{-1/(2\mathrm{i}gt)}\sin(1/(2\sqrt{17}gt)). \quad (12)$$

Notice that $c_1(t)$ and $c_3(t)$ differ from each other only by a sign in one term.

We consider nonperiodic boundary conditions for the particular case of $n = 4$ interacting QED cavities only for the sake of comparison with cavities having periodic ones. However, in the discussion of the results for the nonlocality measure evolution, very interesting issues will be shown to be at play.

2.2 Noninteracting atoms coupled to separate QED cavities

Let us now consider a second model containing a different configuration of atoms and QED cavities. This model is depicted in Fig. 1(b). We again have n two-level atoms $i = 1\cdots n$, each interacting with a single-mode near-resonant cavity field. We assume that each atom–cavity system is isolated and that the cavities are initially in the unexcited state, whereas the atoms are initially in an entangled state.

The model Hamiltonian of the system is given by

$$H = H_0 + H_I = \sum_{i=1}^{n}\nu_i a_i^+ a_i + \frac{\omega_i}{2}\sigma_i^z + \sum_{i=1}^{n} g_i\big(a_i s_i^+ + a_i^+ s_i^-\big), \quad (13)$$

where ω_i and ν_i are the frequencies of the atoms and cavities, respectively. Recall that the only part of the Hamiltonian (13) that will account for a relevant time evolution is H_I.

We consider the atomic degrees of freedom to be in a GHZ-like state, whereas the fields of all the cavities are set to vacuum. Under these conditions, the initial state of the system reads as

$$|\Phi_{ABC..,abc..}(t{=}0)\rangle = \big(\cos\alpha|ggg...g\rangle + \sin\alpha|eee...e\rangle\big) \otimes|000...0\rangle. \quad (14)$$

There are, of course, many other initial configurations, but this one will prove to be quite useful because the results will be given analytically.

Let us suppose again that we deal with a system of $n = 4$ qubits. Now, solving the time-dependent Schrödinger equation in the basis where a total number of excitations n is preserved, as appreciated from the initial state (14), we obtain the following set of differential equations:

$$\begin{aligned}
\mathrm{i}\dot{c_1}(t) &= g_D c_2(t) + g_C c_3(t) + g_B c_5(t) + g_A c_9(t),\\
\mathrm{i}\dot{c_2}(t) &= g_D c_1(t) + g_C c_4(t) + g_B c_6(t) + g_A c_{10}(t),\\
\mathrm{i}\dot{c_3}(t) &= g_C c_1(t) + g_D c_4(t) + g_B c_7(t) + g_A c_{11}(t),\\
\mathrm{i}\dot{c_4}(t) &= g_C c_2(t) + g_D c_3(t) + g_B c_8(t) + g_A c_{12}(t),\\
\mathrm{i}\dot{c_5}(t) &= g_B c_1(t) + g_D c_6(t) + g_C c_7(t) + g_A c_{13}(t),\\
\mathrm{i}\dot{c_6}(t) &= g_B c_2(t) + g_D c_5(t) + g_C c_8(t) + g_A c_{14}(t),\\
\mathrm{i}\dot{c_7}(t) &= g_B c_3(t) + g_C c_5(t) + g_D c_8(t) + g_A c_{15}(t),\\
\mathrm{i}\dot{c_8}(t) &= g_B c_4(t) + g_C c_6(t) + g_D c_7(t) + g_A c_{16}(t),\\
\mathrm{i}\dot{c_9}(t) &= g_A c_1(t) + g_C c_{11}(t) + g_B c_{13}(t) + g_D c_{10}(t),\\
\mathrm{i}\dot{c_{10}}(t) &= g_A c_2(t) + g_D c_9(t) + g_C c_{12}(t) + g_B c_{14}(t),\\
\mathrm{i}\dot{c_{11}}(t) &= g_A c_3(t) + g_C c_9(t) + g_D c_{12}(t) + g_B c_{15}(t),\\
\mathrm{i}\dot{c_{12}}(t) &= g_A c_4(t) + g_C c_{10}(t) + g_D c_{11}(t) + g_B c_{16}(t),\\
\mathrm{i}\dot{c_{13}}(t) &= g_A c_5(t) + g_B c_9(t) + g_D c_{14}(t) + g_C c_{15}(t),\\
\mathrm{i}\dot{c_{14}}(t) &= g_A c_6(t) + g_B c_{10}(t) + g_D c_{13}(t) + g_C c_{16}(t),\\
\mathrm{i}\dot{c_{15}}(t) &= g_A c_7(t) + g_B c_{11}(t) + g_C c_{13}(t) + g_D c_{16}(t),\\
\mathrm{i}\dot{c_{16}}(t) &= g_A c_8(t) + g_B c_{12}(t) + g_C c_{14}(t) + g_D c_{15}(t). \quad (15)
\end{aligned}$$

The set of solutions for each coefficient can be found analytically, with the initial conditions given by $c_i(t = 0) = 0$, $i \in [1, 2^n - 1]$ and $c_{2^n}(t = 0) = \sin\alpha$, where n is the number of atoms. The corresponding solutions for four different cavities, each one containing a single atom, reads as

$$\begin{aligned}
c_1(t) &= \sin(\alpha)\sin(g_A t)\sin(g_B t)\sin(g_C t)\sin(g_D t),\\
c_2(t) &= \mathrm{i}\sin(\alpha)\sin(g_A t)\sin(g_B t)\sin(g_C t)\cos(g_D t,\\
c_3(t) &= \mathrm{i}\sin(\alpha)\sin(g_A t)\sin(g_B t)\cos(g_C t)\sin(g_D t),\\
c_4(t) &= -\sin(\alpha)\sin(g_A t)\sin(g_B t)\cos(g_C t)\cos(g_D t),\\
c_5(t) &= \mathrm{i}\sin(\alpha)\sin(g_A t)\cos(g_B t)\sin(g_C t)\sin(g_D t),\\
c_6(t) &= -\sin(\alpha)\sin(g_A t)\cos(g_B t)\sin(g_C t)\cos(g_D t),\\
c_7(t) &= -\sin(\alpha)\sin(g_A t)\cos(g_B t)\cos(g_C t)\sin(g_D t),\\
c_8(t) &= -\mathrm{i}\sin(\alpha)\sin(g_A t)\cos(g_B t)\cos(g_C t)\cos(g_D t),\\
c_9(t) &= \mathrm{i}\sin(\alpha)\cos(g_A t)\sin(g_B t)\sin(g_C t)\sin(g_D t),\\
c_{10}(t) &= -\sin(\alpha)\cos(g_A t)\sin(g_B t)\sin(g_C t)\cos(g_D t),\\
c_{11}(t) &= -\sin(\alpha)\cos(g_A t)\sin(g_B t)\cos(g_C t)\sin(g_D t),\\
c_{12}(t) &= -\mathrm{i}\sin(\alpha)\cos(g_A t)\sin(g_B t)\cos(g_C t)\cos(g_D t),\\
c_{13}(t) &= -\sin(\alpha)\cos(g_A t)\cos(g_B t)\sin(g_C t)\sin(g_D t),\\
c_{14}(t) &= -\mathrm{i}\sin(\alpha)\cos(g_A t)\cos(g_B t)\sin(g_C t)\cos(g_D t),\\
c_{15}(t) &= -\mathrm{i}\sin(\alpha)\cos(g_A t)\cos(g_B t)\cos(g_C t)\sin(g_D t),\\
c_{16}(t) &= \sin(\alpha)\cos(g_A t)\cos(g_B t)\cos(g_C t)\cos(g_D t). \quad (16)
\end{aligned}$$

The high degree of symmetry of the problem allows us to recover the previous instance $n \to n-1$, in our case $n=3$. To do so, we first set $g_A, c_{9\ldots16}(t) = 0$ in the set of differential equations and then make the replacements $g_B \to g_A$, $g_C \to g_B$, and $g_D \to g_C$. This procedure is possible because of the particular structure and arrangement of the coefficients c_i and coupling constants g_i in the set of differential equations that solves the problem of the evolution of the system.

This particular embedding of the $(n-1)$ problem into the n problem makes it possible to find the general solution to the problem, that is, 2^n differential equations plus the given initial conditions, without the need to solve them explicitly. The only unknown factors are the complex numbers associated with each coefficient. However, these phases are relevant only in the only off-diagonal elements of the reduced density matrix for either the atoms $\rho_{ABCD..}$ or the cavity modes $\rho_{abcd..}$ of the entire system of n QED cavities.

The solution for the problem with $n=3$ atoms, which is encoded in the set of differential equations as explained above, can be retrieved except for a factor $\{1,-1,\mathrm{i},-\mathrm{i}\}$ by making $g_At = \frac{\pi}{2}$ and then applying $g_B \to g_A$, $g_C \to g_B$, $g_D \to g_C$. In fact, the exact solution for $n=3$ is given by

$$\begin{aligned}
c_1(t) &= \mathrm{i}\sin\alpha\sin(g_At)\sin(g_Bt)\sin(g_Ct),\\
c_2(t) &= -\sin\alpha\sin(g_At)\sin(g_Bt)\cos(g_Ct),\\
c_3(t) &= -\sin\alpha\sin(g_At)\cos(g_Bt)\sin(g_Ct),\\
c_4(t) &= -\mathrm{i}\sin\alpha\sin(g_At)\cos(g_Bt)\cos(g_Ct),\\
c_5(t) &= -\sin\alpha\cos(g_At)\sin(g_Bt)\sin(g_Ct),\\
c_6(t) &= -\mathrm{i}\sin\alpha\cos(g_At)\sin(g_Bt)\cos(g_Ct),\\
c_7(t) &= -\mathrm{i}\sin\alpha\cos(g_At)\cos(g_Bt)\sin(g_Ct),\\
c_8(t) &= \sin\alpha\cos(g_At)\cos(g_Bt)\cos(g_Ct). \qquad (17)
\end{aligned}$$

Let us recall that we work in a basis such that the computational states follow the mapping $\{|0\rangle \to |g\rangle, |1\rangle \to |e\rangle\}$. In the general case of n parties, because we are considering only the initial state (14), and bearing in mind that the total number of excitations is preserved (n in total), we can "build" the solution structure for all the coefficients $c_i, i \in [1, 2^n]$ by using the following procedure:

- Given i in c_i, we find the corresponding n digits of the binary expression for $i-1$.
- Next, we make the binary digit 0_k equivalent to $\sin(g_kt)$ and the binary digit 1_k equivalent to $\cos(g_kt)$.
- The resulting structure for the coefficients $c_i(t)$ then reads as

$$\begin{aligned}
c_i &\propto \sin/\cos(g_1t)\cdot\sin/\cos(g_2t)\cdot\sin/\cos(g_3t)\cdot\\
&\quad \sin/\cos(g_4t)\ldots\sin/\cos(g_nt),
\end{aligned}$$

where the proportionality constant can take only the four values $\{1,-1,\mathrm{i},-\mathrm{i}\}\times\sin\alpha$.

For example, if $n=4$ and $k=13$ $(13-1=12 \to 1100)$, we obtain $c_{13}(t) \propto \cos(g_1t)\cos(g_2t)\sin(g_3t)\sin(g_4t)$, and if $n=6$ and $k=51$ $(51-1=50 \to 110010)$, we have $c_{51}(t) \propto \cos(g_1t)\cos(g_2t)\sin(g_3t)\sin(g_4t)\cos(g_5t)\sin(g_6t)$.

A very remarkable property of the general n problem is that the symmetry of the problem entails a result that implies a special type of evolution of the sum of all coefficients $c_i(t)$. In other words, we have the following equation:

$$\mathrm{i}\frac{\mathrm{d}}{\mathrm{d}t}\left(\sum_{i=1}^{2^n} c_i(t)\right) = (g_1+g_2+\ldots+g_n)\left(\sum_{i=1}^{2^n} c_i(t)\right), \quad (18)$$

whose solution

$$\sum_{i=1}^{2^n} c_i(t) = \exp\left(-\mathrm{i}\left[\sum_{j=1}^{n} g_j\right]t\right)\sin\alpha \quad (19)$$

implies a constraint on the sum of all solutions.

To obtain the density matrix for any subsystem choice for the state of n atoms and the modes of n cavities, let us consider for simplicity the case $n=3$. The initial state

$$|\Phi_{ABCabc}(t=0)\rangle = (\cos\alpha|ggg\rangle + \sin\alpha|eee\rangle)\otimes|000\rangle \quad (20)$$

is such that the three atoms can initially be all excited or all in the ground state, but the field modes in each QED cavity are down. This fact implies that three excitations are preserved throughout the evolution of the system as a whole. Therefore, only a subset of all the possible states will evolves. This constraint implies that we can find these states very easily: $c_i(t)$, $i \in [1, 2^{n=3}]$, accompanied by $|i-1\rangle_{\text{atoms}} \otimes |2^{n=3}-(i-1)\rangle_{\text{cavities}}$. The basis for the states of atoms is $\{|ggg\rangle, |gge\rangle, ..., |eee\rangle\}$ and the usual computational basis for the field in the cavities.

By looking at the initial state (20), the ket $|ggg\rangle$ does not evolve, and we have $c_0(t) = \cos\alpha$, whereas the second one does. Therefore, the evolved state looks like

$$\begin{aligned}
|\Phi_{ABCabc}(t)\rangle = c_0|ggg000\rangle &+ c_1|ggg111\rangle + c_2|gge110\rangle\\
&+c_3|geg101\rangle + c_4|gee100\rangle + c_5|egg011\rangle\\
&+c_6|ege010\rangle + c_7|eeg001\rangle + c_8|eee000\rangle. \quad (21)
\end{aligned}$$

At this stage, we define the state $|\Phi_{ABCabc}(t)\rangle\langle\Phi_{ABCabc}(t)|$. If we trace over the field degrees of freedom, we obtain the density matrix for the atomic evolved state alone, which reads, in the basis $\{|ggg\rangle, |gge\rangle, \ldots, |eee\rangle\}$, as

$$\rho_{ABC}(t)=\begin{pmatrix}\cos^2\alpha+|c_1(t)|^2 & 0 & 0 & 0 & 0 & 0 & 0 & \cos\alpha c_8^*(t)\\ 0 & |c_2(t)|^2 & 0 & 0 & 0 & 0 & 0 & 0\\ 0 & 0 & |c_3(t)|^2 & 0 & 0 & 0 & 0 & 0\\ 0 & 0 & 0 & |c_4(t)|^2 & 0 & 0 & 0 & 0\\ 0 & 0 & 0 & 0 & |c_5(t)|^2 & 0 & 0 & 0\\ 0 & 0 & 0 & 0 & 0 & |c_6(t)|^2 & 0 & 0\\ 0 & 0 & 0 & 0 & 0 & 0 & |c_7(t)|^2 & 0\\ \cos\alpha c_8(t) & 0 & 0 & 0 & 0 & 0 & 0 & |c_8(t)|^2\end{pmatrix}. \tag{22}$$

On the other hand, tracing over the state of the atoms, the density matrix for the cavity modes in the basis $\{|000\rangle, |001\rangle, ..., |111\rangle\}$ reads as

$$\rho_{abc}(t)=\begin{pmatrix}\cos^2\alpha+|c_8(t)|^2 & 0 & 0 & 0 & 0 & 0 & 0 & \cos\alpha c_1^*(t)\\ 0 & |c_7(t)|^2 & 0 & 0 & 0 & 0 & 0 & 0\\ 0 & 0 & |c_6(t)|^2 & 0 & 0 & 0 & 0 & 0\\ 0 & 0 & 0 & |c_5(t)|^2 & 0 & 0 & 0 & 0\\ 0 & 0 & 0 & 0 & |c_4(t)|^2 & 0 & 0 & 0\\ 0 & 0 & 0 & 0 & 0 & |c_3(t)|^2 & 0 & 0\\ 0 & 0 & 0 & 0 & 0 & 0 & |c_2(t)|^2 & 0\\ \cos\alpha c_1(t) & 0 & 0 & 0 & 0 & 0 & 0 & |c_1(t)|^2\end{pmatrix}. \tag{23}$$

In light of these results, we can derive two important conclusions. On the one hand, one needs to know only the phase of the complex numbers that accompany $c_8(t)$ (the reduced state for all atoms) and $c_1(t)$ (the reduced state for all field modes), because all the other coefficients appear modulus-squared. On the other hand, we can easily derive the form of the reduced density matrix, say, of n atoms, without having to solve a complex set of ordinary differential equations involving 2^n variables, even numerically.

In addition, a useful quantity, the purity $\mathrm{Tr}(\rho^2)$ for the general case, is not only obtained analytically, but is invariant when considering either only atoms or only field modes as the degrees of freedom considered. That is, in both cases, for those two partitions, the purity $\mathrm{Tr}(\rho^2)$ is the same.

A priori, we do not know whether the purity or the so-called participation ratio $R = 1/\mathrm{Tr}(\rho^2)$ is invariant for any partition we may introduce into the system, mixing both atomic and field degrees of freedom. This question is very important for entanglement transfer. In fact, in Refs. [36, 37], the authors tried, without success, to find an entanglement invariant when correlations are transferred from one particular subsystem to another.

After exploring the different bipartitions of the system, we find that the (inverse) of the participation ratio for both the atomic [(22)] and cavity [(23)] reduced states of n parties is

$$\frac{1}{R}=\left(\cos^4\alpha+\sum_{i=1}^{2^n}|c_i(t)|^4\right)+2\cos^2\alpha(|c_1(t)|^2+|c_{2^n}(t)|^2), \tag{24}$$

which is directly related to the so-called linear entropy $S_L = 1 - 1/R$. Now, after exploring other partitions, we can find counterexamples. Thus, neither R nor S_L is invariant under any possible partition of the system into combinations of atomic and cavity field degrees of freedom. For instance, for the state ρ_{Cab}, the last term in parentheses in (24) for $n = 3$ is $(|c_2(t)|^2+|c_7(t)|^2)$. However, it is remarkable that the first term on the right-hand side of (24) is common to all partitions. Therefore, the only quantity that seems to be *approximately invariant* in the transfer of entanglement from one subsystem to another is $1/R \approx \cos^4\alpha + \sum_{i=1}^{2^n}|c_i(t)|^4$. The reason that $\cos^4\alpha + \sum_{i=1}^{2^n}|c_i(t)|^4$ is invariant is that all the coefficients appear in all the partitions chosen as diagonal matrix elements, in any order, whereas the only differences occur in the only two nonzero off-diagonal matrix elements.

Summing up, we cannot find an entanglement invariant measure either, and there is probably not one. In any case, we managed to find a quantity for our given initial state of the system that is closely related to the purity measure $\mathrm{Tr}(\rho^2)$.

3 Correlation measure employed

One way of characterizing the global degree of entanglement exhibited by an n-qubit state is provided by the sum of the (bipartite) entanglement measures associated with the $2^{n-1}-1$ possible bipartitions of the n-qubit system [38]. This particular number takes into account that the marginal density matrices describing the kth party, after tracing out the rest, are equivalent to those of $n-k$ parties because of the relation $\binom{n}{k}=\binom{n}{n-k}$. In essence, these entanglement measures are given by the degree of mixture of the marginal density matrices associated with each bipartition. In our case, we use the von Neumann entropy

$$S_{\text{total}}=\sum_i -Tr[\rho_i \ln \rho_i], \tag{25}$$

where the sum is performed over all $2^{n-1}-1$ different bipartitions.

However, measure (25) applies only to *pure* states and not to mixed states, which we have here. Thus, we cannot use any proper measure for multipartite entanglement in the mixed-state scenario in a nontrivial way. Measures exist in the literature, but they usually imply the minimization of convex-roof quantities, a numerical procedure that becomes intractable for a high number of qubits.

A good witness of useful correlations is, in many cases, the violation of a Bell inequality by a quantum state. Most of our knowledge of Bell inequalities and their quantum mechanical violation is based on the Clauser–Horne–Shimony–Holt (CHSH) inequality [39]. Let A_1 and A_2 be two possible measurements on the A side whose outcomes are $a_j\in\{-1,+1\}$, and similarly for the B side. Mathematically, it can be shown that $|\mathcal{B}_{CHSH}^{LVM}(\lambda)|=|a_1b_1+a_1b_2+a_2b_1-a_2b_2|\leq 2$. Because a_1 (b_1) and a_2 (b_2) cannot be measured simultaneously, instead one estimates, after randomly chosen measurements, the average value $\mathcal{B}_{CHSH}^{LVM}\equiv\sum_\lambda \mathcal{B}_{CHSH}^{LVM}(\lambda)\mu(\lambda)=E(A_1,B_1)+E(A_1,B_2)+E(A_2,B_1)-E(A_2,B_2)$, where $E(\cdot)$ represents the expectation value. Therefore, the CHSH inequality reduces to $|\mathcal{B}_{CHSH}^{LVM}|\leq 2$.

Quantum mechanically, because we are dealing with qubits, these observables reduce to $\boldsymbol{A}_j(\boldsymbol{B}_j)=\boldsymbol{a}_j(\boldsymbol{b}_j)\cdot\boldsymbol{\sigma}$, where $\boldsymbol{a}_j(\boldsymbol{b}_j)$ are unit vectors in $\mathbb{R}^3$, and $\boldsymbol{\sigma}=(\sigma_x,\sigma_y,\sigma_z)$ are the usual Pauli matrices. Therefore, the quantal prediction for $\mathcal{B}_{CHSH}^{LVM}$ reduces to the expectation value of the operator $\mathcal{B}_{CHSH}=\boldsymbol{A}_1\otimes\boldsymbol{B}_1+\boldsymbol{A}_1\otimes\boldsymbol{B}_2+\boldsymbol{A}_2\otimes\boldsymbol{B}_1-\boldsymbol{A}_2\otimes\boldsymbol{B}_2$.

Although violation of an n-particle Bell-like inequality of some sort by an n-particle entangled state is known to be insufficient *per se* to prove genuine multipartite nonlocality, it is the only approximation left in practice. Mermin, Ardehali, Belinskii, and Klyshko (MABK) inequalities [40–42] are such that they constitute extensions of the CHSH Bell inequalities [39]. To derive an extension to the multipartite case, we introduce a recursive relation [43] that will allow for more parties. This is easily done by considering the operator

$$B_{n+1}\propto[(B_1+B_1')\otimes B_n+(B_1-B_1')\otimes B_n'], \tag{26}$$

where B_n is the Bell operator for n parties, and $B_1=\boldsymbol{v}\cdot\boldsymbol{\sigma}$, where $\boldsymbol{\sigma}=(\sigma_x,\sigma_y,\sigma_z)$, and $\boldsymbol{v}$ is a real unit vector. The prime on the operator denotes the same expression but with all vectors exchanged. The concomitant maximum value

$$MABK_n^{\max}\equiv\max_{\boldsymbol{a}_j,\boldsymbol{b}_j} Tr(\rho B_n) \tag{27}$$

serves as a measure for the nonlocality content of a given state ρ of n qubits if $\boldsymbol{a}_j$ and $\boldsymbol{b}_j$ are unit vectors in $\mathbb{R}^3$. The nonlocality measure (27) is maximized by generalized GHZ states, where $2^{\frac{n+1}{2}}$ is the corresponding maximum value.

However, there exist other measures [44] such as the Svetlichny inequalities [45] that serve the same purpose, as they have a similar structure extended to the n-partite scenario and are identical for n even.

4 Results

Now that we have the evolution of all the reduced states of interest known analytically, we can compute the nonlocality measure in the multipartite case.

4.1 Atoms inside a single cavity

In this case, atoms form a periodic chain inside a single cavity, as illustrated in Fig. 1(a). Although the corresponding state (9) representing the atomic degrees of freedom of the system is analytic for any number of atoms n, we were able to find only approximate expressions for the maximum value of the MABK Bell violation. In any case, we resort to numerical calculations to calculate the nonlocality, which serves the same purpose.

It may be relevant to know the exact form of any reduced state of an individual atom, which is given by

$$\rho_i(t)=\begin{pmatrix} 1-|c_2(t)|^2 & \cos\alpha c_2^*(t) \\ \cos\alpha c_2(t) & |c_2(t)|^2 \end{pmatrix}, \tag{28}$$

with eigenvalues $\lambda^{\pm}=\frac{1}{2}[1\pm\sqrt{1-4|c_2(t)|^2(\sin^2\alpha-|c_2(t)|^2)}]$. For simplicity, we use $\alpha=\frac{\pi}{4}$ in all following calculations related to atoms in one cavity.

4.1.1 n=3

The results for the reduced state of $n=3$ qubits with atomic degrees of freedom are shown in Fig. 2. In Fig. 2(a), the upper curves depict the evolution of the maximum violation of the MABK or Mermin inequality for the periodic arrangement (oscillating curve, in blue) and the open case (curve displayed for all t, in red). Only the open configuration violates the local realism threshold, as shown by the horizontal curve. The bottom curve represents the participation ratio R for the open configuration of three atoms, which departs very little from the pure case ($R = 1$). Notice that there is a correlation between low R values (close to pure states) and optimal maximal violation of the corresponding Mermin inequality. The evolution of the periodic system for the maximum violation of the MABK Bell inequality is depicted in Fig. 2(b) for different values of the ratio J/g. Only two whole periods are depicted.

It is clearly remarkable that the open chain is the only configuration that violates the Mermin inequality, although both the open and periodic ones start with the same uncorrelated state [(2)] for $n = 3$ and $J = g = 1$. The evolution of the open system is known, and the interacting Hamiltonian for the first model [(1)] is the only one responsible for the evolution. The evolution of the maximum violation of the Mermin inequality in Fig. 2(a) is a result of the composition of different harmonic evolutions, as described by the set of coefficients in (12).

Indeed, the only difference that determines whether the corresponding Hamiltonian is an entangling one is fully based on the conditions that are imposed on the interatomic interactions at both ends of the array.

The elucidation of this difference between the open and periodic systems regarding the presence (open system) or absence (periodic system) of nonlocality is not trivial. To explain, at least qualitatively, this nonlocality difference between open and periodic systems, we resort to a comparison with a system that involves entangled chains.

In Ref. [46], the authors imagined an infinite string of qubits such as two-level atoms or the spins of spin-1/2 particles. The string of qubits can be either infinite or a periodic finite ring (equivalent after all), but it cannot be open. There, the authors considered only bipartite entanglement [46], as measured by the concurrence. In this respect, an entangled chain is like an ordinary chain whose links are directly connected only to two neighboring links. They consider two conditions: (i) each qubit is entangled with its nearest neighbors; (ii) the state is invariant under all translations, that is, under transformations that shift each qubit from its original position j to position $j + n$ for some integer n (number of qubits). By virtue of the translational invariance, the degree of (pairwise) entanglement between nearest neighbors in a uniform entangled chain must be constant throughout the chain. Then, the authors proceeded to discuss how large the nearest-neighbor entanglement can be in a uniform entangled chain.

Like this earlier system, our system is periodic, because all the coupling constants between cavities J_i are equal, along with the atomic-field interaction couplings given by g_i. Even though the reduced states for the atomic or cavity mode degrees of freedom are mixed, the restriction to pure states in Ref. [46] entails no loss of generality. Although the density matrix for the atomic evolved state is given in the basis

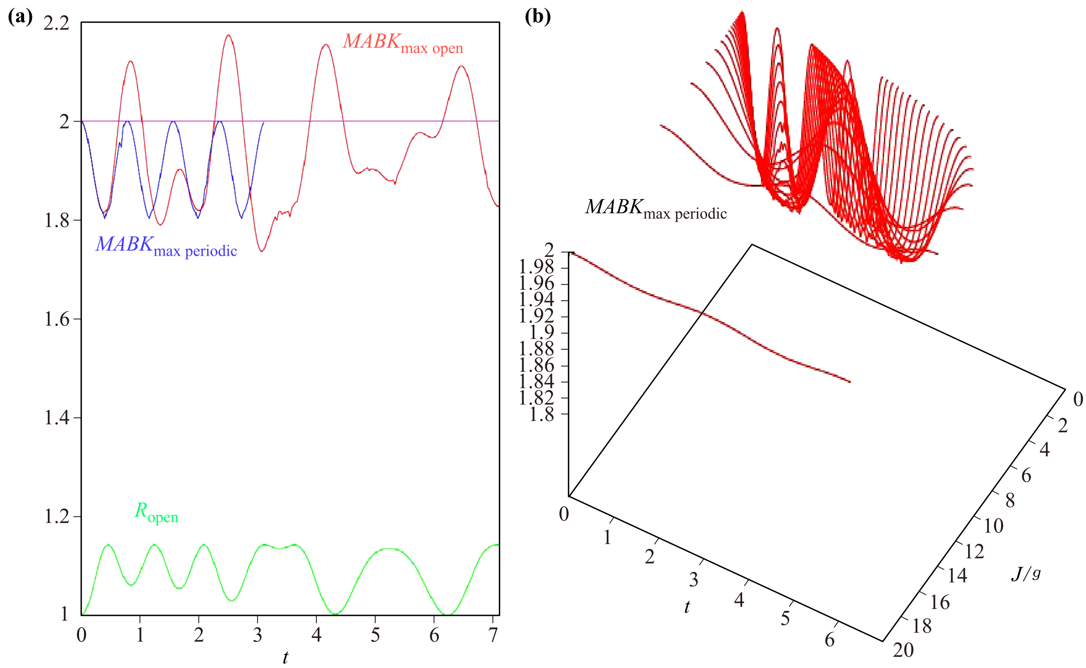

Fig. 2 Plot of multipartite quantum correlation for the first model (1) considered here and $n = 3$. The upper curves in **(a)** represent the maximum violation of the Mermin inequality for the periodic configuration (interval evolution, blue curve) and the open one (whole-range evolution, red curve). The participation ratio R is also depicted at the bottom for the open case. **(b)** depicts the evolution of $MABK_{\max}$ vs. J/g and t for the periodic configuration. See text for details.

$\{|ggg\rangle, |gge\rangle, \ldots, |eee\rangle\}$, which is certainly different from the case considered in Ref. [46], and we use multipartite nonlocality and not bipartite entanglement, we can see that the degree of multipartite nonlocality evolves to values no greater than that corresponding to the initial state. This needs to be a direct consequence of the translational invariance of our system.

Now, when we consider an open system, none of these restrictions apply, and it is plausible to achieve multipartite nonlocality values during the evolution of the system that are *different from* (for example, higher than) those given initially. This fundamental difference in achieving greater values for the multipartite nonlocality as compared to the initial state-value content is interesting *per se* and will be studied in detail elsewhere.

4.1.2 n=6

The evolution for higher instances ($n > 3$) is considered here only for the periodic arrangement of atoms inside the cavity. Although numerical evaluations of (27) are, in general, computationally demanding, for cases such as $n = 6$ they can be performed quite easily. In Fig. 3, we depict the evolution of the maximum violation of the MABK Bell inequality for $n = 6$ qubits and $J = g = 1$. The maximum values are clearly far from even local realism. This is a common feature of the nonlocality measure as we increase the number of parties.

4.1.3 The general n case

The general multipartite nonlocality measure for arbitrary n does not vary much from the previous instances. The participation ratio R, given in the general case by formula (10), indicates how correlations may evolve. Remarkably, R is very close to 1, which entails that the corresponding states are slightly correlated.

In addition, when we fix $J = g = 1$ but make the number of parties variable, the shape of the evolution of R remains basically invariant and only shifts to a higher frequency owing to the dependence of $\Delta = \sqrt{J^2 + ng^2}$ on n, which for large n goes as $O(\sqrt{n})$.

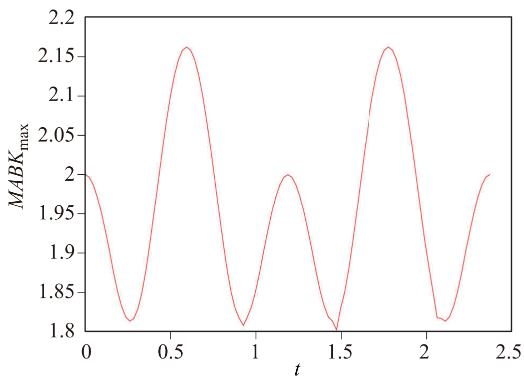

Fig. 3 Plot of the evolution of the maximum violation of the MABK Bell inequality for $n = 6$. See text for details.

If we had a true measure of multipartite entanglement, we might have seen that the states are correlated, even though no nonlocality is present. The reason is the very low value for the degree of mixture and the fact that nonlocality and entanglement represent two different physical resources. As stated before, the presence of quantum correlations (including multipartite entanglement) display a dualistic behavior with the degree of mixture of the corresponding state. Further, it is very likely that for low values of R, the measure of multipartite entanglement may be nonzero regardless of its explicit definition. However, because no such measure can be used for multipartite entanglement, the characterization of the concomitant quantum correlations must be given by the maximum violation of a Bell inequality.

4.2 Atoms inside different cavities

Let us now proceed to calculate nonlocality for the reduced states of n atoms, each of which is placed in a different cavity, as depicted in Fig. 1(b). Nonlocality for both the atomic [(22)] and cavity [(23)] reduced states of n parties can be found analytically, and all the corresponding calculations are shown in detail in the Appendix.

For simplicity, we consider that all the cavities are identical, and therefore $g_i = g \forall i$. In addition, we consider that all the atoms are initially in a GHZ state ($\alpha = \frac{\pi}{4}$), unless otherwise stated. This case will be the most interesting in terms of the evolution of quantum correlations.

4.2.1 n=3

The case of $n = 3$ atoms is the simplest multipartite case. Both the atomic [(22)] and cavity [(23)] reduced states of three parties are given analytically. Recall that having one two-level atom inside n different cavities is tantamount to possessing $2n$ qubits of information. In the exploration of the different partitions of the system in groups of three — $\binom{6}{3} = 20$ in total — we find that two of them exhibit perfect nonlocality transfer. These two partitions correspond to the extreme cases of having only atomic or cavity degrees of freedom. As depicted in Fig. 4, whenever the atomic nonlocality is maximum, the cavity one is minimum, and vice versa.

A mathematical description of this phenomenon is given in the corresponding analytic expressions for $MABK^3_{\max}$ for atoms [(A10)] and cavity modes [(A11)], where the leading term in the former is given by a product of the cos functions, whereas in the latter we have sin functions. It is thus plain that the remaining $20-2 = 18$ partitions involving both atomic and cavity degrees of

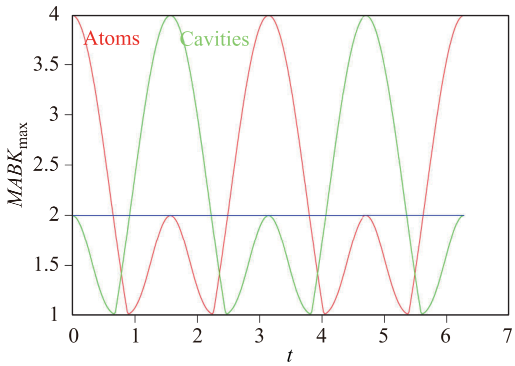

Fig. 4 Evolution of nonlocality $MABK^3_{\max}$ [(A10)] for $g = 1$ and a maximally correlated initial state for three atomic degrees of freedom (red curve) and three cavity degrees of freedom (green curve). Notice the perfect anticorrelation between these two opposite regimes. See text for details.

freedom play a minor role as far as nonlocality transfer is concerned.

We must emphasize that this behavior is not unique to $n = 3$ but is absolutely universal for the general n case. In addition, the situation is worse in terms of the distribution or transfer of quantum correlations because the number of total possible configurations grows very rapidly, that is, $\binom{2n}{n}$.

Further, as the angle α varies between 0 and $\pi/4$, the time evolution highlights several intervals where nonlocality increases and decreases periodically. For initial states that become increasingly correlated, the revivals are more pronounced, and the time lapse between them diminishes slightly. In addition, maximal initial correlation is not necessary for the system to exhibit nonlocality revivals, but it is preferable when decoherence enters the picture.

Once we have obtained $MABK^n_{\max}$ [(A10)] analytically, cases other than the tripartite one behave in a similar way.

4.2.2 The general n case

In contrast to the first model considered in this work, the model with noninteracting cavities whose atoms are initially found in a GHZ-like state is completely analytical as far as the computation of nonlocality is concerned. This fact makes it much easier to properly discuss the properties of the nonlocality revivals that occur for the atomic or cavity degrees of freedom.

Because nonlocality for atoms is given primarily by $2^{\frac{n+1}{2}} \sin 2\alpha \prod_{i=1}^{n} \cos(g_i t) = 2^{\frac{n+1}{2}} \sin 2\alpha |\cos^n(gt)|$, as n grows we have more pronounced oscillation. Likewise, for the cavity case, the cos function must be replaced by the sin function, all else being equal.

As the number of parties increases, the frequency of revivals stays the same and is tuned by the atom–cavity interaction g. However, the widths of the windows in which local realism is violated are reduced, and the nonlocal correlations reappear at very precise times. Thus, to consider a system that can store and retrieve quantum correlations, one must consider a compromise in the total number of cavities or atoms that are initially correlated.

5 Practical limitations on the experimental implementation

Both systems considered here, the one consisting of several atoms inside a single QED cavity and the one with several atoms in QED cavities, constitute a zeroth approximation to the study of quantum correlations in QED cavities. Because we have not modeled any environment, the state of the system does not undergo any decoherence process, and therefore the ensuing evolution is unitary. This is a common limitation for the two systems considered here. How serious is this limitation? Of course, this contribution should consider the unavoidable interaction of the system with the environment. However, under a very controlled environment, we hope these interactions may be minimized so that the main features presented here such as Bell revivals can still be seen.

Assuming that we ignore or can minimize the influence of the environment, let us now list the most serious limitations for each system and how we can cope with them. For the system with several atoms inside a single QED cavity, we have that

- each atom is coupled to the field with the same coupling coefficient g, which is quite impossible in a real experiment. Further, the atom–atom coupling coefficient J is the same for all atoms, which is very difficult to achieve experimentally.

The immediate consequence of this drawback is that the periodic arrangement is no longer interesting. This is so because the translation invariance is violated (the g_i and J_i values are all different). Ironically, we are then forced to consider the system of atoms inside the cavity with open boundary conditions, which we have seen indeed violates the MABK Bell inequalities, at least in the tripartite case. Thus, we may be able to see revivals in nonlocal quantum correlations by changing the architecture of the atoms inside the cavity from periodic to open boundary conditions. Because of the differences in the values of all the coupling constants, the ensuing revivals will have a complex periodic evolution with time.

Now, regarding many noninteracting cavities, each of them with an atom inside, we may have that

- it is extremely hard to keep all the cavities operating under the same conditions.

In other words, maintaining reasonable coherence between cavities can be very challenging. However, as assumed in the case of a minimally tailored environment, coherence between these noninteracting cavities may be maintained for sufficiently long times. In that case, how would the likely difference between the coupling constants g_i affect the idealized results? The fact that we have assumed that all the g_i values are equal implies that the resonances appearing in the nonlocality measure occur at very precise times. Having different g_i values in the general expression $2^{\frac{n+1}{2}} \sin 2\alpha \prod_{i=1}^{n} \cos(g_i t)$ would certainly prevent us from having resonances. However, while it is true that having the same coupling g_i for each atom is difficult, we could still see nonlocality resonances provided that the couplings g_i do not differ greatly from each other. In other words, if one can manage experimentally to provide $g_i = \bar{g} \pm \hat{u}_i$, where $\hat{u}_i$ is a random variable that does not depart much from a mean value $\bar{g}$, nonlocal resonances could still be seen provided the decoherence times are also sufficiently long.

These limitations should be considered for an eventual practical realization, and they must be listed here. However, big things have small beginnings, and therefore we have in this work explored first the potential use of the existing quantum correlations in these systems from an idealized, proof-of-principle point of view.

6 Conclusions

In this contribution, we considered two models of atoms arranged in QED cavities. In the first model, in which all atoms are embedded inside a single cavity, atoms can interact with their nearest neighbors, and all atoms interact with the cavity field with the same strength. We showed how the nonlocality, as well as the entanglement, evolves with time for multiple parties. The corresponding reduced states for the atomic degrees of freedom were obtained analytically for periodic boundary conditions. Regarding whether the system in an open array of atoms or a closed one has physical consequences, we observed that there is a remarkable difference in the case of three qubits, as far as nonlocality is concerned, between the open and periodic cases. In the open case, the evolution is slightly more involved, and there appears to be a concentration of quantum correlations for truly quantum correlations starting from an initial, uncorrelated state. The periodic boundary condition configuration exhibits revivals in nonlocality, but never beyond the locality threshold for three qubits, as opposed to its open counterpart.

In the other model considered, we studied the evolution of nonlocality for a system of n atoms inside different QED cavities, which represent a total of $2n$ qubits considering those of the cavity field modes. Starting with the maximum correlated state for n qubits, we analytically obtained the maximum value of the violation of the MABK Bell inequality, which was thoroughly checked by the numerical method. The capacity to analytically obtain the ensuing reduced states for the atomic degrees of freedom enabled us to study this model in utmost detail.

For the first model, the most striking feature of the system under consideration is that it experiences nonlocality revivals, although in this second model, the initial state is already maximally correlated. These revivals entail sudden death and sudden birth, quite similar to those of quantum entanglement. The capacity to store and periodically provide maximum correlations to the atomic degrees of freedom makes the system attractive for quantum communication purposes. These maximum correlations can be provided at precise times, which are given by a particular tuning of the atom–field coupling constants when all of them are equal. However, the oscillating nature of these revivals is directly related to the number of parties n involved. Thus, the effective time interval in which an ample violation of the MABK Bell inequality occurs depends directly on n. This fact implies that if the system needs to be used as a "correlation reservoir", the total number of parties must be chosen very carefully.

A unique feature of the second model is the total transfer of nonlocality from full atomic degrees of freedom to full cavity field degrees of freedom. A surprising feature is that the maximum transfer occurs in these two extreme cases, and thus, the remaining $\binom{2n}{2} - 2$ possible configurations are disregarded.

The models were presented to see the main differences in terms of the quantum correlations. The closed array of atoms inside a single cavity behaves much like the second model, but there is a fundamental difference due to the interaction between atoms, which is zero in the second model. Thus, the first model (starting with a noncorrelated initial state and interacting atoms) with periodic boundary conditions and the second one (with an initially maximally correlated state and noninteracting atoms/cavities) exhibit similar behavior as far as nonlocality revivals are concerned. This result has interesting echoes in the possible use of cavity-QED arrays (see Ref. [48] and references therein) in devices. Therefore, the second model provides a better way of addressing atoms individually, as they are embedded in different cavities.

However, open arrays of atoms with nearest-neighbor interactions, all of which are coupled to the same QED cavity, experience nonlocality revivals that return correlations that are higher than the initial input. This effect, shown here for the case of three qubits, will certainly be the subject of further research on the general multipartite scenario.

Acknowledgements J. Batle acknowledges fruitful discussions with J. Rosselló, Maria del Mar Batle, and Regina Batle. Further, J. Batle is greatly indebted to Maria Vallespir Socias for her support and understanding.

Appendix A

This appendix derives the maximum violation of the MABK Bell inequality, (26) and (27), for the atomic reduced states of n separate cavities, which is given by the extension of states (22) to the general multiqubit case. Let us first call the set of values $\{\lambda_1, \cdots, \lambda_{2^n}\}$ the diagonal elements corresponding to $\lambda_1 = \cos^2\alpha + |c_1(t)|^2$, $\lambda_i = |c_i(t)|^2$, and $\Delta = \cos\alpha c^*_{2^n}(t)$. Notice that by using this notation, we can also find the maximum violation of the MABK Bell inequality for the cavity mode states of n qubits [the extension of states (23)] by a proper redefinition of the λ variables and Δ.

The present endeavor might be somewhat difficult at first owing to the complex form of the MABK Bell operator (26) as the number of qubits n increases. However, because many entries in the general state are zero, we shall see that it is possible to achieve a closed, compact form even for the general case. The optimization is known to be taken over the two observers' settings $\{\boldsymbol{a}_j, \boldsymbol{b}_j\}$, which are real unit vectors in $\mathbb{R}^3$.

Now, the general form of the MABK operator for $n = 3$, which defines the Mermin inequality $\mathrm{Tr}(\rho\mathcal{B}_{Mermin}) \leq 2$, reads as

$$\mathcal{B}_{Mermin} = B_{a_1a_2a_3} - B_{a_1b_2b_3} - B_{b_1a_2b_3} - B_{b_1b_2a_3}, \quad \text{(A1)}$$

with $B_{uvw} \equiv \boldsymbol{u}\cdot\boldsymbol{\sigma}\otimes\boldsymbol{v}\cdot\boldsymbol{\sigma}\otimes\boldsymbol{w}\cdot\boldsymbol{\sigma}$, where $\boldsymbol{\sigma} = (\sigma_x, \sigma_y, \sigma_z)$ are the usual Pauli matrices, and $\boldsymbol{a}_j$ and $\boldsymbol{b}_j$ are unit vectors in $\mathbb{R}^3$. For $n = 4$ qubits, the MABK operator $\mathcal{B}_{MABK}$, which defines the MABK inequality $Tr(\rho\mathcal{B}_{MABK}) \leq 4$, reads as

$$\begin{aligned} B_{1111} &- B_{1112} - B_{1121} - B_{1211} - B_{2111} - B_{1122} - B_{1212} \\ &- B_{2112} - B_{1221} - B_{2121} - B_{2211} + B_{2222} + B_{2221} \\ &+ B_{2212} + B_{2122} + B_{1222}, \end{aligned}$$

where $B_{uvwx} \equiv \boldsymbol{u}\cdot\boldsymbol{\sigma}\otimes\boldsymbol{v}\cdot\boldsymbol{\sigma}\otimes\boldsymbol{w}\cdot\boldsymbol{\sigma}\otimes\boldsymbol{x}\cdot\boldsymbol{\sigma}$. Notice that we have limited the subindices to 1 and 2, which denote **a** and **b**, respectively, for each qubit in $\boldsymbol{uvwx}$.

Our proof of the maximum violation of the MABK Bell inequality (27) for the atomic reduced states of n separate cavities will be constructive. Before we proceed, let us recall that the total number of terms in the MABK operator is 4^{n-2}, where $n \geq 4$, and thus it may seem a very difficult task to find the solution for any n for states (22). Let us first consider the case for one single entry of the type $\boldsymbol{\alpha}\cdot\boldsymbol{\sigma}\otimes\boldsymbol{\beta}\cdot\sigma$ for $n = 2$ qubits. Writing this in the computational basis $\{|00\rangle, |01\rangle, |10\rangle, |11\rangle\}$, we have

$$\begin{pmatrix} \alpha_z\beta_z & \alpha_z\beta^- & \alpha^-\beta_z & \alpha^-\beta^- \\ \alpha_z\beta^+ & -\alpha_z\beta_z & \alpha^-\beta^+ & -\alpha^-\beta_z \\ \alpha^+\beta_z & \alpha^+\beta^- & -\alpha_z\beta_z & -\alpha_z\beta^- \\ \alpha^+\beta^+ & -\alpha^+\beta_z & -\alpha_z\beta^+ & \alpha_z\beta_z \end{pmatrix}, \quad \text{(A2)}$$

where $\alpha^\pm = \alpha_x \pm \mathrm{i}\alpha_y$, and $\beta^\pm = \beta_x \pm \mathrm{i}\beta_y$. An arbitrary term in the $n = 3$ case is given by

$$\begin{pmatrix} \alpha_z\beta_z & \alpha_z\beta^- & \alpha^-\beta_z & \alpha^-\beta^- \\ \alpha_z\beta^+ & -\alpha_z\beta_z & \alpha^-\beta^+ & -\alpha^-\beta_z \\ \alpha^+\beta_z & \alpha^+\beta^- & -\alpha_z\beta_z & -\alpha_z\beta^- \\ \alpha^+\beta^+ & -\alpha^+\beta_z & -\alpha_z\beta^+ & \alpha_z\beta_z \end{pmatrix} \otimes \begin{pmatrix} \gamma_z & \gamma^- \\ \gamma^+ & -\gamma_z \end{pmatrix}, \quad \text{(A3)}$$

where $\alpha^\pm = \alpha_x \pm \mathrm{i}\alpha_y$, $\beta^\pm = \beta_x \pm \mathrm{i}\beta_y$, and $\gamma^\pm = \gamma_x \pm \mathrm{i}\gamma_y$ are the "raising" and "lowering" terms in the $x-y$ plane.

How do we choose the angles for the unit vector observers' settings? We could choose them to be of the form $(\sin\theta_k\cos\phi_k, \sin\theta_k\sin\phi_k, \cos\theta_k)$, which implies a total of $4n$ angles. However, we can assume without loss of generality that all the measurements occur in the same plane, say the $x-z$ one. By doing so, we reduce the total number of variables from $4n$ to $2n$. We can also reduce the number of angles further, to just n, if $\{\boldsymbol{a_j}, \boldsymbol{b_j}\}$ are conjugate vectors, that is, $\boldsymbol{a_j} = (\cos\theta_j, 0, \sin\theta_j)$, and $\boldsymbol{b_j} = (\cos\theta_j, 0, -\sin\theta_j)$.

Now, the quantity $\mathrm{Tr}(\rho B^{(j)}_{n=3})$ for states ρ (22) and operator $B^{(j)}_{n=3}$, that is, any term in (A1), reads as

$$\begin{aligned} &\lambda_1\alpha_z\beta_z\gamma_z + \Delta\alpha_x\beta_x\gamma_x - \lambda_2\alpha_z\beta_z\gamma_z - \lambda_3\alpha_z\beta_z\gamma_z \\ &+\lambda_4\alpha_z\beta_z\gamma_z - \lambda_5\alpha_z\beta_z\gamma_z + \lambda_6\alpha_z\beta_z\gamma_z + \lambda_7\alpha_z\beta_z\gamma_z \\ &+\Delta^*\alpha_x\beta_x\gamma_x - \lambda_8\alpha_z\beta_z\gamma_z \\ &= f(\lambda)\alpha_z\beta_z\gamma_z + g(\Delta)\alpha_x\beta_x\gamma_x, \end{aligned} \quad \text{(A4)}$$

where $f(\lambda) = \lambda_1 - \lambda_2 - \lambda_3 + \lambda_4 - \lambda_5 + \lambda_6 + \lambda_7 - \lambda_8$, and $g(\Delta) = 2\mathrm{Re}(\Delta)$. Because $c_{2^n}(t) = \sin\alpha\prod_{i=1}^n\cos(g_it)$ is always real [the angle α here belongs to the initial pure state (14) and is not to be confused with the same angle in the definition of the MABK Bell operators], we have that $g(\Delta) = 2\cos\alpha c_8(t)$. Likewise, we consider the modulus of $c_{2^n}(t)$.

Adding all the terms in (A4) with appropriate $\{\alpha, \beta, \gamma\}$ in the four contributions in (A1), with $\boldsymbol{a_1}/\boldsymbol{b_1} = (\cos\alpha, 0, \pm\sin\alpha)$, $\boldsymbol{a_2}/\boldsymbol{b_2} = (\cos\beta, 0, \pm\sin\beta)$, and $\boldsymbol{a}_3/\boldsymbol{b}_3 = (\cos\gamma, 0, \pm\sin\gamma)$, we obtain

$$\begin{aligned} \mathrm{Tr}(\rho B_{n=3}) = -2\big[&f(\lambda)\sin\alpha\sin\beta\sin\gamma \\ &+g(\Delta)\cos\alpha\cos\beta\cos\gamma\big]. \end{aligned} \quad \text{(A5)}$$

The optimization of this quantity over the angles $\{\alpha, \beta, \gamma\}$ is found to be

$$MABK^{n=3}_{\max} = \max\left(2|f(\lambda)|, 4|g(\Delta)|\right). \quad \text{(A6)}$$

The numerical maximization of the nonlocality $MABK_{\max}$ for any number of qubits n requires an exploration among their corresponding unit vectors defining the observers' settings. In the necessary cases, we performed a two-fold search employing (i) an amoeba optimization procedure, where the optimal value is obtained at the risk of falling into a local minimum and (ii) the well-known simulated annealing approach [47]. The advantage of this dual computational approach is that we can be confident regarding the final results reached. Indeed, the second recipe contains a mechanism that allows for local searches that can eventually escape local optima.

After the numerical survey was carefully performed, the agreement with the analytic result (A6) was excellent.

With the previous example provided for the $n = 3$ case, we can now proceed to generalize. First, the most difficult part is to find the list of correct signs in $f(\lambda)$, which contains the sums of the diagonal terms in states (22) for any n. Recall that these terms are gathered when collecting all the factors that multiply only the products of the z contributions. The construction from one operator for n qubits to the next one, $n+1$, is clearly given by the tensor product (A3). We use it in the following quadrants in the angular sense. The new operator will contain the previous one multiplied by a new (positive) z factor in the II quadrant. Likewise, those for the I and III quadrants will contain the previous one multiplied by a new (positive) x factor. It will be the II quadrant that will be changed in the sign, given by the same (now negative) z factor. Because this procedure is repeated iteratively, positive and negative signs will appear. We start with $\{1, -1, -1, 1\}$, the diagonal signs for the two-qubit operator (A3). The other half of the diagonal elements will be just the previous ones with their sign changed, and we proceed again. The list of signs of the terms that multiply the diagonal elements for the general n case $\lambda_{i=1\cdots 2^n}$ can be retrieved by applying the following simple algorithm:

```
vsign(1) = 1
vsign(2) = -1
vsign(3) = -1
vsign(4) = 1
do inq = 3, n
    do i = 2^(inq-1) + 1, 2^inq
        vsign(i) = -vsign(i - 2^(inq-1))
    end do
end do
return vsign array.                                        (A7)
```

Thus, the final value for each sign of the sum in $f(\lambda)$ is given in the position of the array vsign(). Regarding the term multiplying $g(\Delta)$, the upper-right element for every ensuing operator in (A3) will always be a product of the x factors, with $g(\Delta) = 2\cos\alpha c_{2^n}(t)$.

Therefore, one generic element $\mathrm{Tr}(\rho B_n)$ of the existing 4^{n-2} reads as

$$f(\lambda)\prod_{j=1}^{n}\sin\theta_j + g(\Delta)\prod_{j=1}^{n}\cos\theta_j. \tag{A8}$$

To proceed, we need to know the sign of all the 4^{n-2} contributions to the general MABK quantity that will be optimized. For instance, for $n = 3$, 3 are negative and 1 is positive (balance -2), and for $n = 4$, 10 are negative and 6 are positive (balance -4). In light of the construction given in definition (26), it is very easy to show by induction that the nth balance is twice the previous one. Therefore, the overall number of negative plus positive terms is equal to 2^{n-2} times the number of *negative* terms.

Gathering all the previous results, we obtain

$$\mathrm{Tr}(\rho B_n) = -2^{n-2}\big[f(\lambda)\prod_{j=1}^{n}\sin\theta_j + g(\Delta)\prod_{j=1}^{n}\cos\theta_j\big], \tag{A9}$$

whose maximization returns

$$MABK^n_{\max} = \max\big(2|f(\lambda)|, 2^{\frac{n+1}{2}}|g(\Delta)|\big). \tag{A10}$$

The maximum value at which the MABK Bell inequalities are violated is given by the second term, $2^{\frac{n+1}{2}}|g(\Delta)|$, that is, $2^{\frac{n+1}{2}}2\cos\alpha\sin\alpha\prod_{i=1}^{n}\cos(g_i t)$. In other words, the nonlocality measure is given by $2^{\frac{n+1}{2}}\sin 2\alpha\prod_{i=1}^{n}|\cos(g_i t)|$, which, at certain times, is found above the locality threshold.

By the same token, the expression for the maximum violation of the MABK Bell inequalities for the states (23) that represent the cavity field degrees of freedom can be obtained similarly. We now have to take into account that the sum of the diagonal terms in (23) and higher-n states, which gives rise to $f(\lambda)$, has the same sign rule as before, but λ_i now corresponds to $|c_{2^n-i+1}(t)|^2$. For the cavity degrees of freedom, $g(\Delta)$ is given by $2\cos\alpha|c_1(t)|$.

Therefore, the maximum violation of the MABK Bell inequality for any number of cavities n is expressed as

$$MABK^n_{\max} = \max\big(2|f(\lambda)|, 2^{\frac{n+1}{2}}|g(\Delta)|\big), \tag{A11}$$

where the leading contribution is that of $2^{\frac{n+1}{2}}\sin 2\alpha\prod_{i=1}^{n}|\sin(g_i t)|$.

References

1. H.-K. Lo, S. Popescu, and T. Spiller, Introduction to Quantum Computation and Information, Singapore: World Scientific, 1998

2. A. Galindo and M. A. Martín-Delgado, Information and computation: Classical and quantum aspects, *Rev. Mod. Phys.* 74(2), 347 (2002)
3. M. A. Nielsen and I. L. Chuang, Quantum Computation and Quantum Information, Cambridge: Cambridge University Press, 2000
4. C. P. Williams and S. H. Clearwater, Explorations in Quantum Computing, New York: Springer, 1997
5. C. P. Williams, Quantum Computing and Quantum Communications, Berlin: Springer, 1998
6. C. H. Bennett, G. Brassard, C. Crepeau, R. Jozsa, A. Peres, and W. K. Wootters, Teleporting an unknown quantum state via dual classical and Einstein–Podolsky–Rosen channels, *Phys. Rev. Lett.* 70(13), 1895 (1993)
7. C. H. Bennett and S. J. Wiesner, Communication via one- and two-particle operators on Einstein–Podolsky–Rosen states, *Phys. Rev. Lett.* 69(20), 2881 (1992)
8. A. Ekert and R. Jozsa, Quantum computation and Shor's factoring algorithm, *Rev. Mod. Phys.* 68(3), 733 (1996)
9. G. P. Berman, G. D. Doolen, R. Mainieri, and V. I. Tsifrinovich, Introduction to Quantum Computers, Singapore: World Scientific, 1998
10. J. Batle and M. Casas, Nonlocality and entanglement in the XY-model, *Phys. Rev. A* 82(6), 062101 (2010)
11. J. Batle and M. Casas, Nonlocality and entanglement in qubit systems, *J. Phys. A Math. Theor.* 44(44), 445304 (2011)
12. N. Gisin, Bell's inequality holds for all non-product states, *Phys. Lett. A* 154(5–6), 201 (1991)
13. B. Schumacher, Bell's theorem and monogamy, See: http://pirsa.org/08120020/
14. J. Barrett, L. Hardy, and A. Kent, No signaling and quantum key distribution, *Phys. Rev. Lett.* 95(1), 010503 (2005)
15. A. Acín, N. Gisin, and L. Masanes, From Bell's theorem to secure quantum key distribution, *Phys. Rev. Lett.* 97, 120405 (2006)
16. A. Acín, N. Brunner, N. Gisin, S. Massar, S. Pironio, and V. Scarani, Device-independent security of quantum cryptography against collective attacks, *Phys. Rev. Lett.* 98(23), 230501 (2007)
17. C. Brukner, M. Zukowski, and A. Zeilinger, Quantum communication complexity protocol with two entangled qutrits, *Phys. Rev. Lett.* 89(19), 197901 (2002)
18. P. R. Berman (Ed.), Cavity Quantum Electrodynamics, San Diego: Academic, 1994
19. H. J. Kimble, Strong interactions of single atoms and photons in cavity QED, *Phys. Scr.* T76(1), 127 (1998)
20. J. M. Raimond, M. Brune, and S. Haroche, Manipulating quantum entanglement with atoms and photons in a cavity, *Rev. Mod. Phys.* 73(3), 565 (2001)
21. H. Mabuchi and A. C. Doherty, Cavity quantum electrodynamics: Coherence in context, *Science* 298(5597), 1372 (2002)
22. S. Haroche and J.M. Raimond, Exploring the Quantum: Atoms, Cavities, and Photons, Oxford: Oxford University Press, 2006
23. E. T. Jaynes and F. W. Cummings, Comparison of quantum and semiclassical radiation theories with application to the beam maser, *Proc. IEEE* 51(1), 89 (1963)
24. A comprehensive review on the Jaynes–Cummings model is given in: B. W. Shore and P. L. Knight, The Jaynes–Cummings model, *J. Mod. Opt.* 40, 1195 (1993)
25. A. Rauschenbeutel, G. Nogues, S. Osnaghi, P. Bertet, M. Brune, J. M. Raimond, and S. Haroche, Coherent operation of a tunable quantum phase gate in cavity QED, *Phys. Rev. Lett.* 83(24), 5166 (1999)
26. A. D. Boozer, A. Boca, R. Miller, T. E. Northup, and H. J. Kimble, Reversible state transfer between light and a single trapped atom, *Phys. Rev. Lett.* 98(19), 193601 (2007)
27. M. Koch, C. Sames, M. Balbach, H. Chibani, A. Kubanek, K. Murr, T. Wilk, and G. Rempe, Three-photon correlations in a strongly driven atom-cavity system, *Phys. Rev. Lett.* 107(2), 023601 (2011)
28. A. Reiserer, C. Nölleke, S. Ritter, and G. Rempe, Ground-state cooling of a single atom at the center of an optical cavity, *Phys. Rev. Lett.* 110(22), 223003 (2013)
29. C. Sames, H. Chibani, C. Hamsen, P. Altin, T. Wilk, and G. Rempe, Antiresonance phase shift in strongly coupled cavity QED, *Phys. Rev. Lett.* 112, 043601
30. N. Kalb, A. Reiserer, S. Ritter, and G. Rempe, Heralded storage of a photonic quantum bit in a single atom, *Phys. Rev. Lett.* 114, 220501 (2015)
31. T. Pellizzari, S. A. Gardiner, J. I. Cirac, and P. Zoller, Decoherence, continuous observation, and quantum computing: A cavity QED model, *Phys. Rev. Lett.* 75, 3788 (1995)
32. S. J. van Enk, J. I. Cirac, and P. Zoller, Purifying two-bit quantum gates and joint measurements in cavity QED, *Phys. Rev. Lett.* 79, 5178 (1997)
33. J. Pachos and H. Walther, Quantum computation with trapped ions in an optical cavity, *Phys. Rev. Lett.* 89, 187903 (2002)
34. L. M. Duan, A. Kuzmich, and H. J. Kimble, Cavity QED and quantum-information processing with "hot" trapped atoms, *Phys. Rev. A* 67, 032305 (2003)
35. X. X. Yi, X. H. Su, and L. You, Conditional quantum phase gate between two 3-state atoms, *Phys. Rev. Lett.* 90, 097902 (2003)
36. M. Yönaç, T. Yu, and J. H. Eberly, Sudden death of entanglement of two Jaynes–Cummings atoms, *J. Phys. B: At. Mol.Opt. Phys.* 39, 621 (2006)
37. I. Sainz and G. Björk, Entanglement invariant for the double Jaynes–Cummings model, *Phys. Rev. A* 76, 042313 (2007)

38. I. D. K. Brown, S. Stepney, A. Sudbery, and S. L. Braunstein, Searching for highly entangled multi-qubit states, *J. Phys. A: Math. Gen.* 38, 1119 (2005)
39. J. F. Clauser, M. A. Horne, A. Shimony, and R. A. Holt, Proposed experiment to test local hidden-variable theories, *Phys. Rev. Lett.* 23, 880 (1969)
40. N. D. Mermin, Extreme quantum entanglement in a superposition of macroscopically distinct states, *Phys. Rev. Lett.* 65, 1838 (1990)
41. M. Ardehali, Bell inequalities with a magnitude of violation that grows exponentially with the number of particles, *Phys. Rev. A* 46, 5375 (1992)
42. A. V. Belinskii and D. N. Klyshko, Interference of light and Bell's theorem, *Phys. Usp.* 36(8), 653 (1993)
43. N. Gisin and H. Bechmann-Pasquinucci, Bell inequality, Bell states and maximally entangled states for n qubits, *Phys. Lett. A* 246(1–2), 1 (1998)
44. V. Scarani, A. Acín, E. Schenck, and M. Aspelmeyer, Nonlocality of cluster states of qubits, *Phys. Rev. A* 71, 042325 (2005)
45. G. Svetlichny, Distinguishing three-body from two-body nonseparability by a Bell-type inequality, *Phys. Rev. D* 35, 3066 (1987)
46. K. M. O'Connor and W. K. Wootters, Entangled rings, *Phys. Rev. A* 63, 052302 (2001)
47. S. Kirkpatrick, C. D. Gelatt Jr, and M. P. Vecchi, Optimization by simulated annealing, *Science* 220(4598), 671 (1983)
48. A. Tomadin and R. Fazio, Many-body phenomena in QED-cavity arrays, *J. Opt. Soc. Am. B* 27, 130 (2010)